PAPER TITLE: EFFECT OF LOAD AND STRESS ANALYSIS OF AN ISOTROPIC RECTANGULAR PLATE

1. Onyeka, F. C.
Affiliation: *Department of Civil Engineering, Edo University, Iyamho. Edo State, Nigeria.*
Email: *onyeka.festus@edouniversity.edu.ng*

2. Okeke Thompson Edozie
Affiliation: *Department of Civil Engineering, University of Nigeria, Nsukka, Nigeria.*
Email: *edozie.okeke@unn.edu.ng*

ABSTRACT: In this work, static bending analysis of an isotropic rectangular plate subjected to uniform distributed transverse loads is presented using displacement and refined shear deformation theory. This theory, which is based on traditional higher-order shear deformation is applied in a bending analysis of a rectangular plate. Total potential energy equation of a thick plate is formulated from the static elastic theory of the plate. The coefficient of deflection and shear deformation were derived by subjection the total potential energy obtained to direct variation. The objective of this study is to develop formula's for calculation of the critical lateral imposed load of the plate before deflection reaches the specified maximum specified limit q_{iw} and critical lateral imposed load before plate reaches an elastic yield point q_{ip}. By solving the formulated expression, the effect of stress and load distribution analysis of a mild steel rectangular plates with one edge clamped and free and the other opposite edge simply supported (csfs) and clamped supported at second and fourth edge, simply supported at first edge and free of support at third edge (scfc) were analysed and compared. The essence is to ensure that deflection does not exceed specified maximum limit and the plate shear not exceeding the elastic yielding point. Furthermore, this approach overcomes the challenges of the conventional practice in the structural analysis/design which involves checking of deflection and shear; the process which is proved unreliable. It is concluded that the values of critical lateral load obtained by this theory achieve accepted transverse shear stress to the thickness of plate variation and satisfied the vertical flexibility of condition of the plate while predicting the bending behavior of an isotropic rectangular csfs and scfc plate.

Keywords: *CSFS plates, SCFC plate, shear deformation plate theory, direct variation, and critical lateral imposed load.*

1. INTRODUCTION

The importance of plate structures in aerospace, aeronautic, automotive, military and structural engineering cannot be overemphasized. In structural engineering, they can be used as bridge deck, retaining wall for water retaining structures, panel for building slab, ship hull and spacecraft. Isotropic plates refer to plates whose material properties in all directions at a point are same while anisotropic or orthotropic plates refer to plates whose material properties are direction dependent. With increasing use of isotropic plate material, the need for an improved approach for load analysis is now easily discovered. In such materials, the transverse shear stresses and strains which were induced by the applied load intensification affect the bending characteristics. To analyze the bending due to the applied load, the value of the critical load which efficiently causes the plate structure to be unstable as per equilibrium should be developed and evaluated. Critical Load is defined as the highest loading value, which will not cause any lateral deflection or tangential deflection on the structure. When the critical load exceeds the design load of the structure, it will be in deflecting position [14]. As the load is increased beyond the critical load the lateral deflections increase, until it may fail in other modes such as yielding of the material [16]. To avoid failure happening within the structural member, analytical approach to bending behavior is necessary.

Since the classical plate theory (CPT) [17-18], which did not account for transverse shear effects proved unsatisfactory when applied to the isotropic plate analysis with large shear stress, shear deformation theory is obligatory.

Many shear deformation theories have been developed by many researchers; Reddy, Sayyad and Ghugal [3-6, 7-8, 9] developed a more accurate solution which considers the effect of shear deformation (TSDT, HSDT and ESDT respectively) to predict the bending and free vibration behavior of thick isotropic plates under uniformly distributed lateral load.

In [6], the authors applied the trigonometric shear deformation theory (TSDT) for the analysis of rectangular plates. Their theory and others [1- 4] incorporates the effect of transverse shear stress and shear deformation in the analysis. Results obtained using the above theory shows slight errors in predicting responses of the lateral load on the structures.

Polynomial displacement functions [16] can be applied successfully to solve CCCC and CCFC

boundary condition of thick rectangular plate; a feat that could not be easily achieved using trigonometric, hyperbolic and exponential shape functions. It will contribute in addressing the problem of dearth of literature on the function of polynomial displacement functions. Scholars and practicing engineers will assess, apply and sustain trust in their works/designs. Thereby the psychological trauma due to doubt or not too sure of ones works using Fourier series to analyze thick plates will be done away with.

In [15], the authors used the polynomial shear deformation theory (PSDT) for the analysis of rectangular plates. Their theory incorporates the effect of transverse shear stress and shear deformation in the analysis. Results obtained using the theories did not introduce much error in the analysis, but it ended up determining the displacements, moments and stresses that may occur due to the applied load without obtaining the critical lateral load in predicting responses of the applied load which can lead to failure on the structures.

In [16], the authors used nonlinear strain–displacement polynomial shape function of third order shear deformation theory for rectangular thick plate analysis under uniformly distributed load. They determine imposed load that causes deflection of rectangular plates with all four edges clamped (CCCC) and plate with free of support at third edge and the other edges clamped (CCFC) rectangular thick, but did not obtain for other type of plate.

In this work, the static bending analysis of an isotropic rectangular plate subjected to uniform distributed transverse loads was presented using displacement and refined shear deformation theory. This theory which is based on traditional higher-order shear deformation was applied in a bending analysis of rectangular plate with one edge clamped and free and the other opposite edge simply supported (csfs) and clamped supported at second and fourth edge, simply supported at first edge and free of support at third edge (scfc) to determine effect of stress and load distribution analysis on an isotropic rectangular plate.

2. DISPLACEMENT AND CONSTITUTIVE RELATIONS

The elastic plate under lateral loading as shown in Figure 1 was used to obtain the displacement – strain relationships in terms of curvatures.

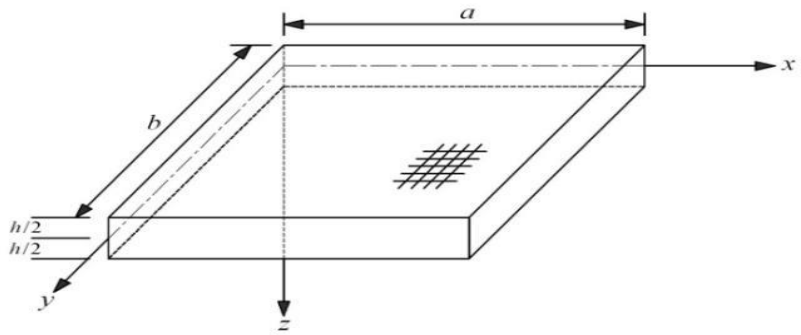

Figure 1: Rectangular plate under bending subjected to uniformly distributed load

The deflection and in – plane displacement functions $(w,\ v\ and\ u)$ of the plate were obtained from the displacement-strain relations and stress-strain relations. Taking a rectangular plate subjected to uniformly distributed load as shown in Figure 1, the corresponding relationship was demonstrated by applying hooks law.

The inplane displacement components along x-axis and inplane displacement components along y axis as presented in the equation (1.0) and (2.0) respectively:

$$u = \frac{zdw}{dy} + F.\theta_{sX} \quad (1)$$

$$v = \frac{zdw}{dy} + F.\theta_{sy} \quad (2)$$

Where:

$F = F(z)\ and\ w = w(x, y)$

$$F(z) = \frac{3}{2}\left(z - \frac{4z^3}{3t^2}\right)\ (see\ [13]) \quad (3)$$

Where:

the symbol u denotes inplane displacement in x axis

the symbol v denotes inplane displacement in y axis

the symbol w denotes deflection

the symbol $F(z)$ denotes Shear deformation profile
the symbol θ_{Sx} denotes shear deformation rotation along x axis
the symbol θ_{Sy} denotes shear deformation rotation along y axis

The three displacements of thick place assumed to involve the deflection, w(x,y) and the two inplane displacements, u(x,y,z), and v(x,y,z) was used to establish the constitutive equations of the rectangular plate.

The constitutive equations for five stress components are:

$$\sigma_x = \frac{Ez}{1-\mu^2}\left(\left(\frac{-d^2w}{dx^2} + \frac{Fd\theta_{Sx}}{dx}\right) + \mu\left(\frac{d^2w}{dy^2} + \frac{Fd\theta_{Sx}}{dy}\right)\right) \quad 4$$

$$\sigma_y = \frac{Ez}{1-\mu^2}\left(\left(-\frac{d^2w}{dy^2} + \frac{Fd\theta_{Sx}}{dx}\right) + \mu\left(\frac{d^2w}{dx^2} + \frac{Fd\theta_{Sx}}{dy}\right)\right) \quad 5$$

Also, from known state Equation,

$$\tau_{xy} = \frac{E(1-\mu)}{(1-\mu^2)}\left(-\frac{z\partial^2w}{\partial x\partial y} + F\left(\frac{d\theta_{Sx}}{dy} + \frac{d\theta_{Sy}}{dx}\right)\right) \quad 6$$

Similarly,

$$\tau_{xz} = \frac{E(1-\mu)}{(1-\mu^2)}\left(\frac{z\partial^2w}{\partial x\partial z} + F\left(\frac{d\theta_{Sx}}{dz} + \frac{d\theta_{Sz}}{dx}\right)\right) \quad 7$$

Also,

$$\tau_{yz} = \frac{E(1-\mu)}{(1-\mu^2)}\left(\frac{z\partial^2w}{\partial y\partial z} + F\left(\frac{d\theta_{Sy}}{dz} + \frac{d\theta_{Sz}}{dy}\right)\right) \quad 8$$

$$\therefore\ \sigma_x = \frac{E\left(\varepsilon_x + \mu\varepsilon_y\right)}{1-\mu^2} \quad 9$$

Similarly reasoning in y direction, we obtain:

$$\sigma_y = \frac{E\left(\varepsilon_y + \mu\varepsilon_x\right)}{1-\mu^2} \quad 10$$

Similarly reasoning in z direction, we obtain:

$$\sigma_z = \frac{E(\varepsilon_z + \mu\varepsilon_x)}{1-\mu^2} \quad 11$$

Similarly;

$$\tau_{xy} = \frac{E}{2(1+\mu)}\cdot\gamma_{xy}$$

$$\tau_{xz} = \frac{E}{2(1+\mu)}\cdot\gamma_{xz} \quad 12$$

$$\tau_{yz} = \frac{E}{2(1+\mu)}\cdot\gamma_{yz} \quad 13$$

Where:
the symbol μ denotes poison ratio
the symbol E denotes modulus of elasticity of the plate
the symbol σ_x denotes stress normal to x axis
the symbol σ_y denotes stress normal to y axis
the symbol τ_{xy} denotes shear stress along x-y axis
the symbol τ_{xz} denotes shear stress along x-z axis
the symbol τ_{yz} denotes shear stress along y-z axis

3. DIRECT GOVERNING ENERGY EQUATION

The direct variational method is used to obtain the direct governing differential equation by differentiating the total potential energy with respect to the coefficient of deflection A_s, coefficient of shear deformation with respect to x-axis A_x and coefficient of shear deformation with respect to y-axis A_y.
The total potential energy functional (Π), the deflection and in – plane displacement functions $(w,\ v\ and\ u)$ of thick isotropic plate were derived [13], as;

$$\Pi = U + V \quad 14$$

given that $U\ and\ V$ are the strain energy and external work respectively, let;

$$V = -\int_0^a \int_0^b qw(x,y)\partial x\partial y \quad (15)$$

Where;

q is the uniformly distributed load

$$U = \frac{1}{2}\iiint_{-\frac{t}{2}}^{\frac{t}{2}} (\sigma_x\varepsilon_{x+}\sigma_y\varepsilon_{y+}\tau_{xy}\gamma_{xy} + \tau_{xz}\gamma_{xz} + \tau_{yz}\gamma_{yz})dxdydz \quad (16)$$

Where:

the symbol ε_x denotes normal strain along x axis

the symbol ε_y denotes normal strain along y axis

the symbol γ_{xy} denotes shear strain along x-y axis

the symbol γ_{xz} denotes shear strain along x-z axis

the symbol γ_{yz} denotes shear strain along y-z axis

Substituting the values of $\sigma_x,\ \varepsilon_{x,}\ \sigma_{y,}\ \varepsilon_{y,}\ \tau_{xy,}\ \gamma_{xy}, \tau_{xz}, \gamma_{xz}, \tau_{yz}, and\ \gamma_{yz}$ into Equation 16 gives:

$$\begin{aligned}\Pi = \frac{D}{2}\int_0^a \int_0^b \Bigg[\Bigg| & g_1\left(\frac{\partial^2 w}{\partial x^2}\right)^2 - 2g_2\left(\frac{\partial^2 w}{\partial x^2}.\frac{\partial \theta_{Sx}}{\partial x}\right) + g_3\left(\frac{\partial \theta_{Sx}}{\partial x}\right)^2\Bigg| \\ & + \left|2g_1\left(\frac{\partial^2 w}{\partial x\partial y}\right)^2 - 2g_2\left(\frac{\partial^2 w}{\partial x\partial y}.\frac{\partial \theta_{Sx}}{\partial y}\right) - 2g_2\left(\frac{\partial^2 w}{\partial x\partial y}.\frac{\partial \theta_{Sy}}{\partial x}\right)\right| \\ & + \left|(1+\mu)g_3\left(\frac{\partial \theta_{Sx}}{\partial y}\right)\left(\frac{\partial \theta_{Sy}}{\partial x}\right)\right| + \frac{(1-\mu)}{2}\left|g_3\left(\frac{\partial \theta_{Sx}}{\partial y}\right)^2 + g_3\left(\frac{\partial \theta_{Sy}}{\partial x}\right)^2\right| \\ & + \left|g_1\left(\frac{\partial^2 w}{\partial y^2}\right)^2 - 2g_2\left(\frac{\partial^2 w}{\partial y^2}.\frac{\partial \theta_{Sy}}{\partial y}\right) + g_3\left(\frac{\partial \theta_{Sy}}{\partial y}\right)^2\right| \\ & + \left|\frac{(1-\mu)}{2}g_4(\theta_{Sx})^2 + \frac{(1-\mu)}{2}g_4\left(\theta_{Sy}\right)^2\right|\Bigg]\partial x\partial y - \int_0^a \int_0^b qw(x,y)\partial x\partial y \end{aligned} \quad (17)$$

given that D is the Rigidity, let;

$$D = \frac{Et^3}{12(1-\mu^2)} \quad (18)$$

$$g_1 = \left(\frac{t^3}{12}\right).\left(\frac{12}{t^3}\right) \equiv 1 \quad (19)$$

$$g_2 = 1.5.\left(\frac{12}{15}\right) \equiv 1.2 \quad (20)$$

$$g_3 = 1.5.\left(1 - \frac{3}{27}\right) \equiv 1.33 \quad (21)$$

$$g_4 = \left(1.5\left(\frac{d\left(\frac{3t^2z - 4z^3}{3t^2}\right)}{dz}\right)^2\right)_{\frac{-t}{2}}^{\frac{t}{2}}.\left(\frac{12}{t^3}\right) = 14.4 \quad (22)$$

4. Direct Governing Equation

The direct variational technique is utilized to obtain the direct governing differential equation by differentiating the total potential energy with respect to the coefficient of deflection A_s, coefficient of shear deformation with respect to x-axis, A_x and coefficient of shear deformation with respect to y-axis, A_y.

The non-dimensional values of quantities along the x- and y-axis respectively is presented as follows, let:

$$x = aR \text{ and } y = bQ \quad (23)$$

The length to breath aspect ratio is

$$\propto = \frac{b}{a} \quad (24)$$

and the span to thickness ratio is

$$\rho = \frac{a}{t} \quad (25)$$

The deflection, *w* is the product of shape function of the plate and deflection coefficient, expressed as:

$$w = h.A_s \quad (26)$$

*A*s is the coefficient of deflection and *h* is the plate shape function.

The shear deformation rotation along the x-axis and y-axis, respectively become:

$$\theta_{Sx} = \left[\frac{dh}{dR}\right][A_x] \quad (27)$$

$$\theta_{sy} = \left[\frac{dh}{dQ}\right][A_y] \quad (28)$$

Given Ax and Ay are the shear deformation along x and y axis respectively. By substituting equations (18), (23), (24), (25), (26) and (27) into Eq. (17), gives Eq. (29).

$$\begin{aligned}\Pi = \frac{Et^3}{24(1-\mu^2)a^4}\int_0^1\int_0^1 \Bigg[\Bigg| & g_1 {A_s}^2\left(\frac{\partial^2 h}{\partial R^2}\right)^2 - 2g_2 A_s A_x\left(\frac{\partial^2 h}{\partial R^2}\right)^2 + g_3 {A_x}^2\left(\frac{\partial^2 h}{\partial R^2}\right)^2\Bigg| \\ & + \left|2g_1\frac{{A_s}^2}{\propto^2}\left(\frac{\partial^2 h}{\partial R\partial Q}\right)^2 - 2g_2\frac{A_s A_x}{\propto^2}\left(\frac{\partial^2 h}{\partial R\partial Q}\right)^2 - 2g_2\frac{A_s A_y}{\propto^2}\left(\frac{\partial^2 h}{\partial R\partial Q}\right)^2\right| \\ & + \left|(1+\mu)g_3\frac{A_x A_y}{\propto^2}\left(\frac{\partial^2 h}{\partial R\partial Q}\right)^2\right| + \frac{(1-\mu)}{2}\left|g_3\frac{{A_x}^2}{\propto^2}\left(\frac{\partial^2 h}{\partial R\partial Q}\right)^2 + g_3\frac{{A_y}^2}{\propto^2}\left(\frac{\partial^2 h}{\partial R\partial Q}\right)^2\right| \\ & + \left|g_1\frac{{A_s}^2}{\propto^4}\left(\frac{\partial^2 h}{\partial Q^2}\right)^2 - 2g_2\frac{A_s A_y}{\propto^4}\left(\frac{\partial^2 h}{\partial Q^2}\right)^2 + g_3\frac{{A_y}^2}{\propto^4}\left(\frac{\partial^2 h}{\partial Q^2}\right)^2\right| \\ & + \left|\frac{(1-\mu)}{2}\rho^2 g_4 {A_x}^2\left(\frac{\partial h}{\partial R}\right)^2 + \frac{(1-\mu)}{2}.\frac{\rho^2 g_4 {A_y}^2}{\propto^2}\left(\frac{\partial h}{\partial Q}\right)^2\right|\Bigg] ab\partial R\partial Q \\ & - \int_0^1\int_0^1 qA_s h\, ab\partial R\partial Q \end{aligned} \quad (29)$$

Thus, differentiating the total potential energy equation (Eq. (29)) with respect to A_s, A_x and A_y, gives:

$$\frac{\partial\Pi}{\partial A_s} = \frac{\partial\Pi}{\partial A_x} = \frac{\partial\Pi}{\partial A_y} = 0 \quad (30)$$

Gives:

$$\begin{bmatrix} r_{11} & r_{12} & r_{13} \\ r_{21} & r_{22} & r_{23} \\ r_{31} & r_{32} & r_{33}\end{bmatrix}\begin{bmatrix} A_s \\ A_x \\ A_y\end{bmatrix} = \frac{qa^4}{D}\begin{bmatrix} k_q \\ 0 \\ 0\end{bmatrix} \quad (31)$$

Let:

$$r_{11} = g_1\left(k_1 + \frac{2}{\propto^2}k_2 + \frac{1}{\propto^4}k_3\right) \quad (32)$$

$$r_{12} = -g_2\left(k_1 + \frac{1}{\propto^2}k_2\right) \quad (33)$$

$$r_{13} = -g_2\left(\frac{1}{\propto^2}k_2 + \frac{1}{\propto^4}k_3\right) \quad (34)$$

$$r_{21} = -g_2\left(k_1 + \frac{1}{\propto^2}k_2\right) \quad (35)$$

$$r_{22} = \left(g_3 k_1 + \frac{(1-\mu)}{2\propto^2}g_3 k_2 + \frac{(1-\mu)}{2}\rho^2 g_4 k_4\right) \quad (36)$$

$$r_{23} = g_3\frac{(1+\mu)}{2\propto^2}k_2 \quad (37)$$

$$r_{31} = -g_2\left(\frac{1}{\propto^2}k_2 + \frac{1}{\propto^4}k_3\right) \quad (38)$$

$$r_{32} = g_3 \frac{(1+\mu)}{2 \propto^2} k_2 \quad (39)$$

$$r_{33} = \left(g_3 \frac{(1-\mu)}{2} \left(\frac{1}{\propto^2} k_2 + \frac{1}{\propto^4} k_3 \right) + g_4 \frac{(1-\mu)}{2 \propto^2} \rho^2 k_5 \right) \quad (40)$$

And;

$$k_1 = \int_0^1 \int_0^1 \left(\frac{d^2h}{dR^2} \right)^2 dRdQ \quad (41a)$$

$$k_2 = \int_0^1 \int_0^1 \left(\frac{d^2h}{dRdQ} \right)^2 dRdQ \quad (41b)$$

$$k_3 = \int_0^1 \int_0^1 \left(\frac{d^2h}{dQ^2} \right)^2 dRdQ \quad (41c)$$

$$k_4 = \int_0^1 \int_0^1 \left(\frac{dh}{dR} \right)^2 dRdQ \quad (41d)$$

$$k_5 = \int_0^1 \int_0^1 \left(\frac{dh}{dQ} \right)^2 dRdQ \quad (41e)$$

$$k_q = \int_0^1 \int_0^1 h.dRdQ \quad (41f)$$

Thus;

$$T_2 = \frac{r_{21}.r_{33} - r_{23}.r_{31}}{r_{22}.r_{33} - r_{23}.r_{32}} \quad (42a)$$

$$T_3 = \frac{r_{21}.r_{32} - r_{22}.r_{31}}{r_{23}.r_{32} - r_{22}.r_{33}} \quad (42b)$$

And Therefore;

$$A_s = \frac{qa^4}{D} \left(\frac{k_q}{r_{11}T_1 - r_{12}T_2 - r_{13}T_3} \right) \quad (43)$$

That is:

$$A_s = \frac{qa^4}{D} \left(\frac{k_q}{r_{11} - r_{12}T_2 - r_{13}T_3} \right) \quad (44)$$

Where

$$T_1 = 1 \quad (45)$$

Recall;

$$A_s = \frac{qa^4}{D}(k) \quad (46)$$

Where;

$$D = \frac{Et^3}{12(1-\mu^2)} \quad (47)$$

$$k = \frac{k_q}{k_T} \quad (48)$$

$$k_T = k_1 + \frac{2}{\propto^2} k_2 + \frac{1}{\propto^4} k_3 \quad (49)$$

5. FORMULATION OF THE CRITICAL LATERAL IMPOSED LOAD IN THE RECTANGULAR PLATE

The formulae for calculating the critical imposed load before deflection reaches specified maximum limit, q_{iw} and its corresponding critical lateral imposed load of the plate before plate reaches elastic yield stress, q_{ip} is developed using equation established from the previous sections.

To ensure that the critical lateral load the plate is determined before it reaches yielding, recall that;

$$w = A_s \mathrm{h} < \mathrm{w_a} \quad (50)$$

$$\frac{12(1-\mu^2)qa^4}{Et^3} . \left(\frac{k_q}{r_{11} - r_{12}T_2 - r_{13}T_3} \right) . \mathrm{h} < \mathrm{w_a} \quad (51)$$

where,

w_a = Allowable deflection
given that *w*a is the allowable deflection. Let,

$$q = \gamma + q_{iw} \quad (52)$$

This gives:

$$q_{iw} < Et^3 \frac{w_a (r_{11} - r_{12}T_2 - r_{13}T_3)}{(1-\mu^2)12.k_q.ha^4} - \gamma \quad (53)$$

where;
γ = Self weight of the plate
And,
q_{iw} = Critical Imposed load of the plate
Also, to ensure that the critical lateral load the plate is determined before it reaches yielding; recall that:

$$U = \frac{1}{2}\iiint_{-\frac{t}{2}}^{\frac{t}{2}} \cap dxdydz \quad (54)$$

where;

$$\cap = \sigma_x\varepsilon_{x+}\sigma_y\varepsilon_{y+}\tau_{xy}\gamma_{xy} + \tau_{xz}\gamma_{xz} + \tau_{yz}\gamma_{yz} \quad (55)$$

Therefore:

$$\cap = \frac{1}{E}\left[\sigma_x{}^2 - \mu\sigma_x\sigma_y - \mu\sigma_x\sigma_y + \sigma_y{}^2 + 2(1+\mu)\tau_{xy}{}^2 + 2(1+\mu)\tau_{xz}{}^2 + 2(1+\mu)\tau_{yz}{}^2\right] \quad (56)$$

This gives:

$$\cap = \frac{1}{E}\left[\sigma_x{}^2 - \mu\sigma_x\sigma_y - \mu\sigma_x\sigma_y + \sigma_y{}^2 + 2(1+\mu)\tau_{xy}{}^2 + 2(1+\mu)\tau_{xz}{}^2 + 2(1+\mu)\tau_{yz}{}^2\right] < \cap_0 \quad (57)$$

Let:

$$\varepsilon_X = \frac{\sigma_X - \mu\sigma_Y}{E} \quad (58)$$

$$\varepsilon_Y = \frac{\sigma_Y - \mu\sigma_X}{E} \quad (59)$$

$$\gamma_{xy} = \frac{2(1+\mu)\tau_{xy}}{E} \quad (60)$$

Similarly,

$$\gamma_{xy} = \frac{2(1+\mu)\tau_{xz}}{E} \quad (61)$$

Also,

$$\gamma_{yz} = \frac{2(1+\mu)\tau_{yz}}{E} \quad (62)$$

$\cap_0$= yielding point of the plate.
For a bar,
$let\ \sigma_X = fy\ and\ \sigma_Y = \tau_{xy} = \tau_{xz} = \tau_{yz} = 0$
Therefore;

$$\cap < \cap_0 > \frac{fy^2}{E} \quad (63)$$

Putting Equation 57 into 63; we have:

$$\frac{1}{E}\left[\sigma_x{}^2 - 2\mu\sigma_x\sigma_y + \sigma_y{}^2 + 2(1+\mu)\tau_{xy}{}^2 + 2(1+\mu)\tau_{xz}{}^2 + 2(1+\mu)\tau_{yz}{}^2\right] < \frac{fy^2}{E} \quad (64)$$

Let,

$$\sigma_Y = n_1\sigma_x \quad (65)$$

$$\tau_{xy} = n_2\sigma_x \quad (66)$$

$$\tau_{xz} = n_3\sigma_x \quad (67)$$

$$\tau_{yz} = n_4\sigma_x \quad (68)$$

Therefore, substituting Equations 65, 66, 67 and 68 into 64, we have:

$$\sigma_x < \frac{fy}{\left[1 - 2\mu n_1 + n_1{}^2 + 2(1+\mu)n_2{}^2 + 2(1+\mu)n_3{}^2 + 2(1+\mu)n_4{}^2\right]} \quad (69)$$

By simplifying equation 1 and 6, the value of σ_x becomes;

$$\sigma_x = \frac{12.qa^2}{t^3}.\frac{k_q}{k_T}z\left(\frac{d^2h}{dR^2} + \frac{\mu}{\alpha^2}\frac{d^2h}{dQ^2}\right) \quad (70)$$

By equating equation o 69 and 70, we have:

$$\frac{12.qa^2.k_q}{k_T t^3}.z\emptyset_2 < \frac{fy}{\emptyset_3} \quad (71)$$

This gives:

$$\sigma_x < \frac{fy}{\emptyset_3} \quad (72)$$

This gave:

$$\sigma_x = \frac{qa^4 Ez\emptyset_2}{(1-\mu^2)D \propto^2} . \left(\frac{k_q}{r_{11}T_1 - r_{12}T_2 - r_{13}T_3}\right) \quad (73)$$

Recall,

$$A_1 = \frac{qa^4}{D}\left(\frac{k_q}{r_{11}T_1 - r_{12}T_2 - r_{13}T_3}\right) \quad (74)$$

Let;

$$\emptyset_2 = \left(\frac{d^2h}{dR^2} + \frac{\mu}{\propto^2}\frac{d^2h}{dQ^2}\right) \quad (75)$$

and,

$$\emptyset_3 = \sqrt{\left[1 - 2\mu n_1 + {n_1}^2 + 2(1+\mu){n_2}^2 + 2(1+\mu){n_3}^2 + 2(1+\mu){n_4}^2\right]} \quad (76)$$

From Equation 71, we get expression for q as:

$$q < \frac{fyt^3}{12.a^2.k.z.\emptyset_2.\emptyset_3} \quad (77)$$

Let;

$$q = q_{\,d} + q_{\,ip} \quad (78)$$

Substituting Equation 78 into 77 gives:

$$q_{\,ip} < \frac{fyt^3}{12.a^2.\frac{k_q}{k_T}.z.\emptyset_2.\emptyset_3} - q_{\,d} \quad (79)$$

This gives:

$$q_{\,ip} < \frac{k_T fyt^3}{12.a^2.k_q.z.\emptyset_2\emptyset_3} - \gamma t \quad (80)$$

$q_{\,ip}$ = critical imposed lateral load before plate reach yield stress; fy = strength

i is the specific thickness and qd is the self-weight of the plate and;

$q_{\,d}$ = Self weight of the plate

6. NUMERICAL PROBLEM

The particular shape function for rectangular plate with their respective boundary is shown in figure 2 and figure

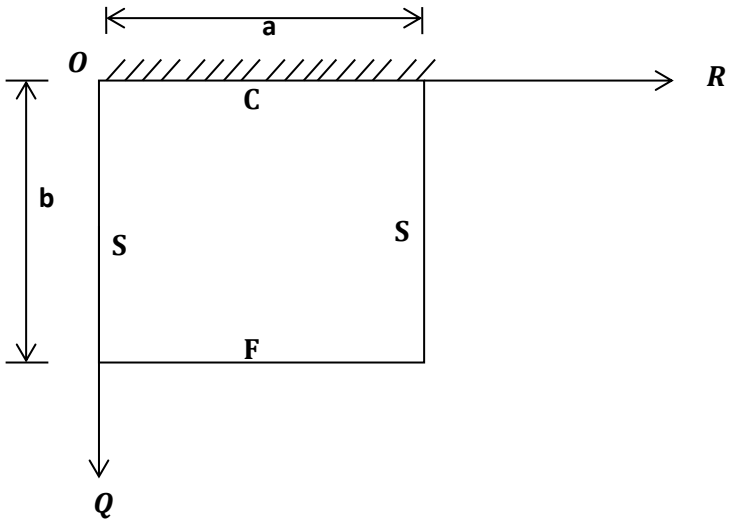

Figure 2: CSFS Rectangular Plate

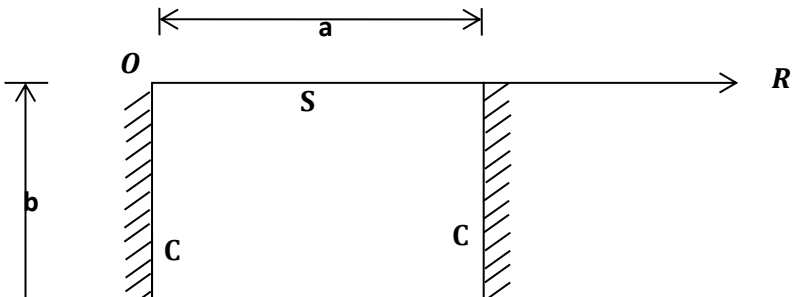

Figure 3: SCFC Rectangular

Considering the figure 2 and 3, the numerical analysis of CSFS and SCFC rectangular plate at various span-thickness ratios are presented in Figure 4 to 10 and Figure 11 to 14 respectively.

A fourth order polynomial displacement function for the analysis CSFS plate was derived as presented in Equation 81:

$$w = (F_{a4}.b_5)\left[(R^2 - 2R^3 + R^4) \times \left(\frac{7Q}{3} - \frac{10}{3}Q^3 + \frac{10}{3}Q^4 - Q^5\right)\right]/8640 \quad 81$$

Let the amplitude,

$$A_s = \frac{(F_{a4} \times F_{b4})}{8640} \quad 82$$

And shape function;

$$h = (R^2 - 2R^3 + R^4) \times \left(\frac{7Q}{3} - \frac{10}{3}Q^3 + \frac{10}{3}Q^4 - Q^5\right) \quad 83$$

Also, a fourth order polynomial displacement function for SCFC plate was derived for the analysis as presented in Equation 84:

$$w = \frac{F_{a4} \times b_5}{8640}(R - 2R^3 + R^4) \times (2.8Q^2 - 5.2Q^3 + 3.8Q^4 - Q^5) \quad 84$$

Let the amplitude,

$$A_s = \frac{F_{a4} \times b_5}{8640} \quad 85$$

And shape function;

$$h = (R - 2R^3 + R^4) \times (2.8Q^2 - 5.2Q^3 + 3.8Q^4 - Q^5) \quad 86$$

2.3.2. Direct Governing Equation

The direct variational technique is utilized to obtain the direct governing differential equation by differentiating the total potential energy with respect to the coefficient of deflection A_s, coefficient of shear deformation with respect to x-axis, A_x and coefficient of shear deformation with respect to y-axis, A_y.

The non-dimensional values of quantities along the x- and y-axis respectively is presented as follows, let:

$$x = aR \text{ and } y = bQ \quad 87$$

The length to breath aspect ratio is

$$\propto = \frac{b}{a} \quad 88$$

and the span to thickness ratio is

$$\rho = \frac{a}{t} \quad 89$$

The deflection, *w* is the product of shape function of the plate and deflection coefficient, expressed as:

$$w = h.A_s \quad 90$$

*A*s is the coefficient of deflection and *h* is the plate shape function.

The shear deformation rotation along the x-axis and y-axis, respectively become:

6. RESULTS AND DISCUSSIONS

The values of stiffness coefficient $(k_1, k_2, k_3, k_4, k_5 \text{ and } k_q)$ obtained from Eq. (41a) to Eq. (41f) are presented in Table 1.

Table 1: Values of Stiffness Coefficient, k for Various Support (boundary conditions)

TYPE	PLATE	k_1	k_2	k_3	k_4	k_5	k_q
1	CSFS	0.3284779	0.0919002	0.1286676	0.0332388	0.00931015	0.0453
2	SCFC	0.6709636	0.0405139	0.0060469	0.0159754	0.00337617	0.0278

From the numerical analysis obtained as presented in the figure 4 to 14, it is if found that as the specified thickness (t) of plate increases, the value of critical lateral imposed load (q_{iw} and q_{ip}) increases. This implies that as we increase the thickness of the plate safety is ensured in the plate structure.

Figure 4 to 14 presents the result of CSFS plate with span of 1000mm, 3000mm and 5000mm at allowable deflection of 1mm, 3mm and 5mm at 5mm, 7.5mm, 10mm, 12.5mm and 15mm specified thickness. From the result, the value of q_{iw} and q_{ip} is between -1.1446 N/mm to 53.413 N/mm and -0.1335 N/mm to 68.517 N/mm been the highest and lowest value at respectively. From the Figure, it is seen that the values of critical lateral imposed load q_{iw} and q_{ip} decrease as the length-width ratio increases, this continues until failure occur. This showed that the greatest failure ($at\ -1.1446$ N/mm) occur at span to breadth ratio and allowable thickness of 2 and 15mm respectively. This means that an increase in plate length increases the chance of failure in a plate structure.

Looking closely at Figure 4 (CSFS plate with span of 1000mm at allowable deflection (w_a) value between 1mm to 5mm). It is found that failure of critical lateral imposed load (q_{iw}) only occur at thickness of 5mm which is between length to width ratio of 1.1, 1.2, 1.3, 1.4, 1.5, 1.6, 1.8, 1.9 and 2 only with value of -0.0266N/mm, -0.0582N/mm, 0.0808N/mm, -0.0976N/mm, -0.01103N/mm, -0.1202N/mm, -0.1280N/mm, -0.1343N/mm, -0.1395N/mm and -0.1438N/mm.

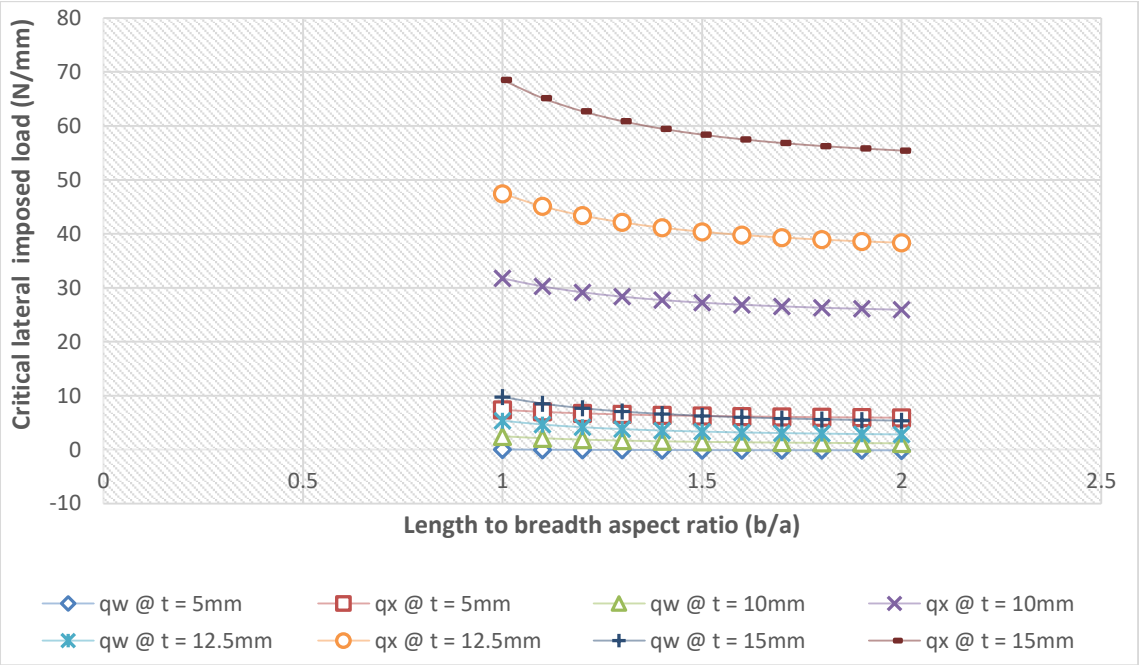

Figure 4: Graph of critical lateral imposed load versus length to breadth ratio of CSFS plate for span, a = 1000mm at $w_a = 1.0$mm

Looking closely at Figure 5 to 7 (CSFS plate with a span of 3000mm at allowable deflection (w_a) value between 1mm to 5mm). It is found that failure of critical lateral imposed load (q_{iw}) only occur at thickness of 1mm and 5mm which is between length to width ratio of 1, 1.1, 1.2, 1.3, 1.4, 1.5, 1.6, 1.8, 1.9 and 2 for all specified thickness value. This shows that the value of critical lateral imposed load (q_{iw}), while the critical imposed load (q_{ip}) remains positive (safe). This means that an increase in the value of the specified deflection failure tendency of the plate structure.

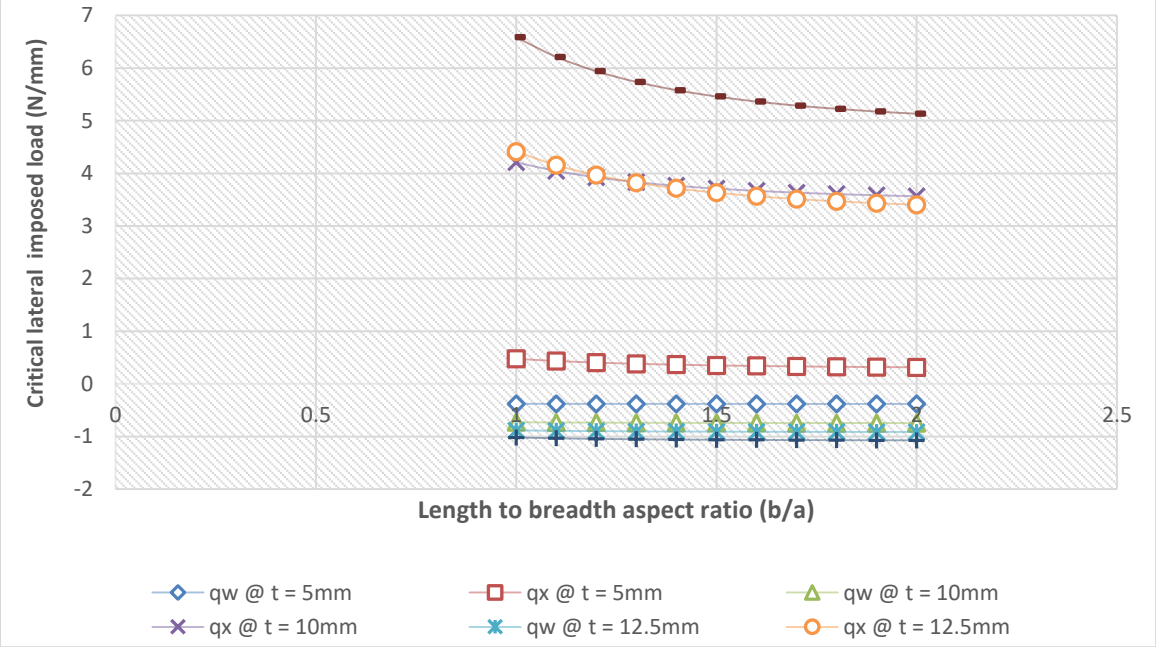

Figure 5: Graph of critical lateral imposed load versus length to breadth ratio of CSFS plate for span, a = 3000mm at $w_a = 1.0$mm

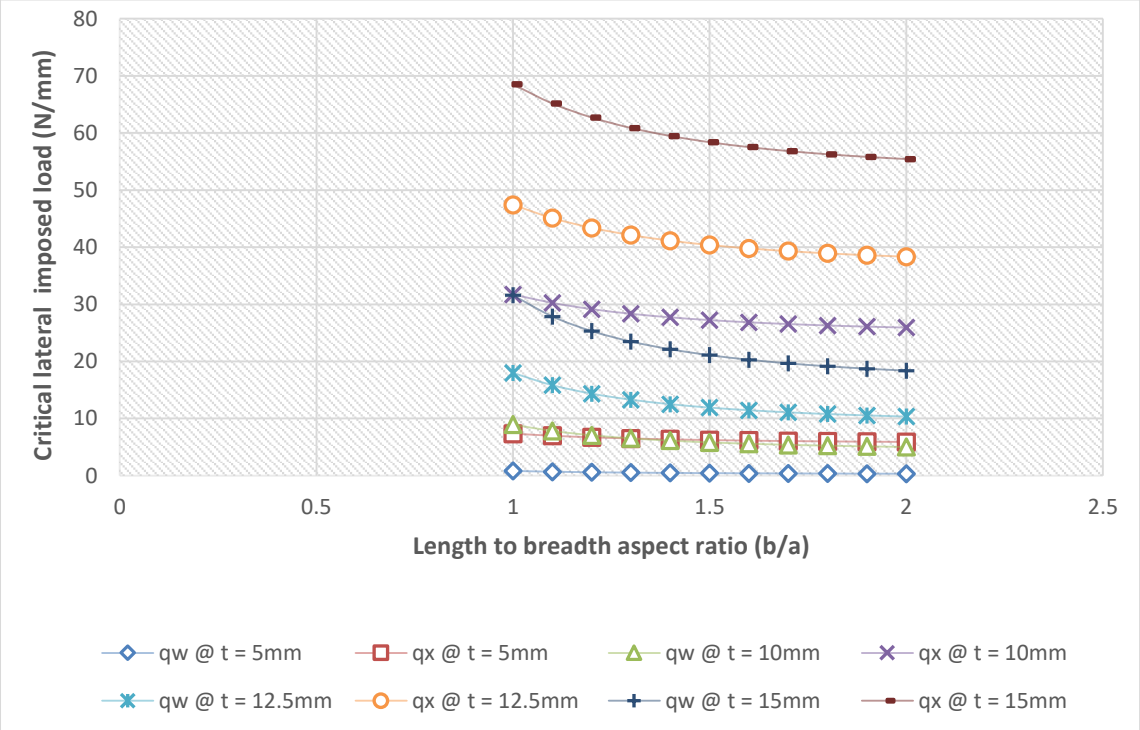

Figure 6: Graph of critical lateral imposed load versus length to breadth ratio of CSFS plate for span, a = 3000mm at $w_a = 3.0$mm

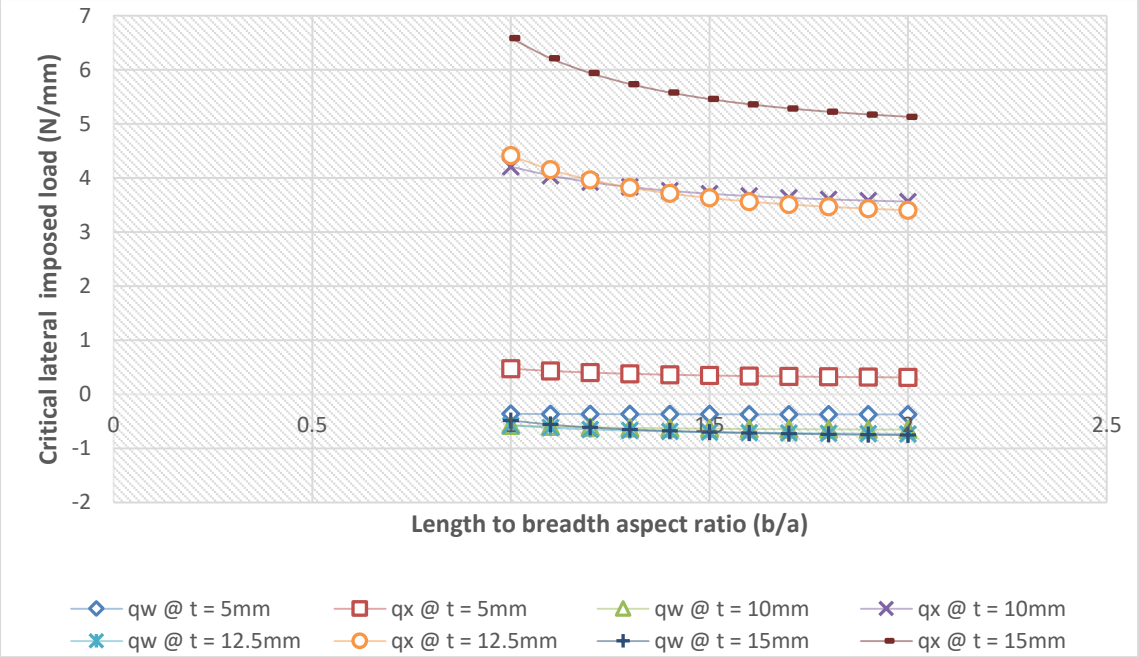

Figure 7: Graph of critical lateral imposed load versus length to breadth ratio of CSFS plate for span, a = 3000mm at $w_a = 5.0mm$

Looking closely at Figure 8 to 10 (CSFS plate with span of 5000mm at allowable deflection (w_a) value between 1mm to 5mm). It is found that failure of critical lateral imposed load (q_{iw} *and* q_{ip}) occur at specified thickness 5mm and 7.5mm which is between length to width ratio of 1, 1.1, 1.2, 1.3, 1.4, 1.5, 1.6, 1.8, 1.9 and 2 for all allowable deflection value while critical lateral imposed load (q_{iw}) only occur at other thickness at all length to width ratio and allowable deflection. The negative value of critical lateral imposed load q_{iw} (and positive value of q_{ip}) only reveals that the plate fails in q_{iw} for the entire plate w_a (1mm to 5mm) and span of 1000mm to 5000mm. This means that the plate structure is not safe and required maintenance. The negative value of critical lateral imposed load (q_{iw} *and* q_{ip}) reveals that the plate fails in both q_{iw} q_{iw} for the entire plate w_a (1mm to 5mm) for all types of plate. This means the total failure plate structure and this lead to collapse.

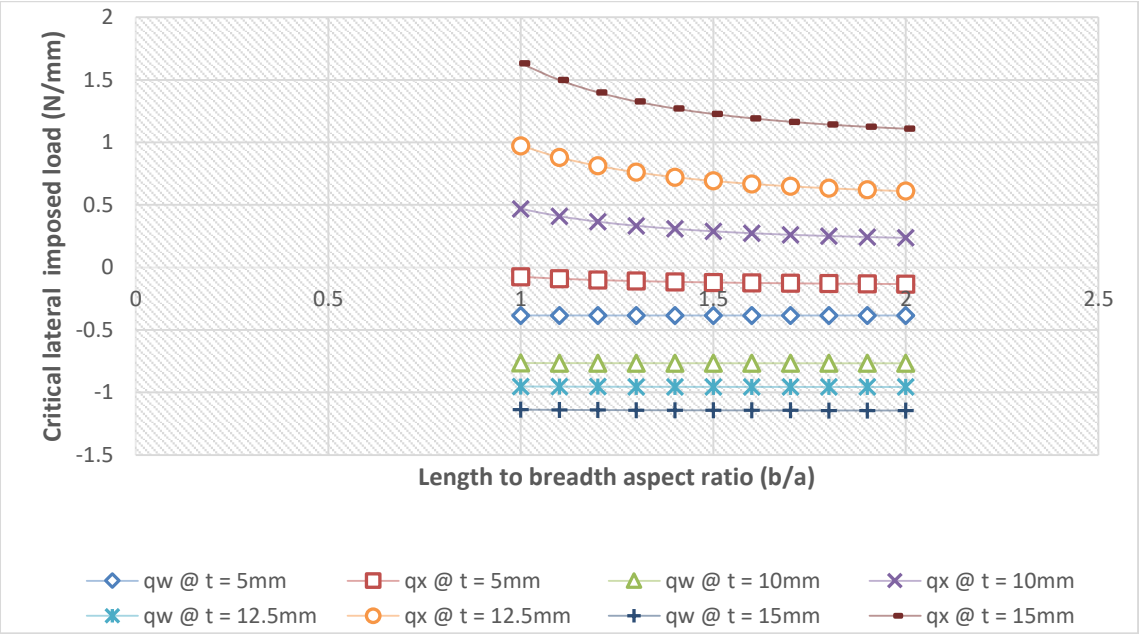

Figure 8: Graph of critical lateral imposed load versus length to breadth ratio of CSFS plate for span, a = 5000mm at $w_a = 1.0mm$

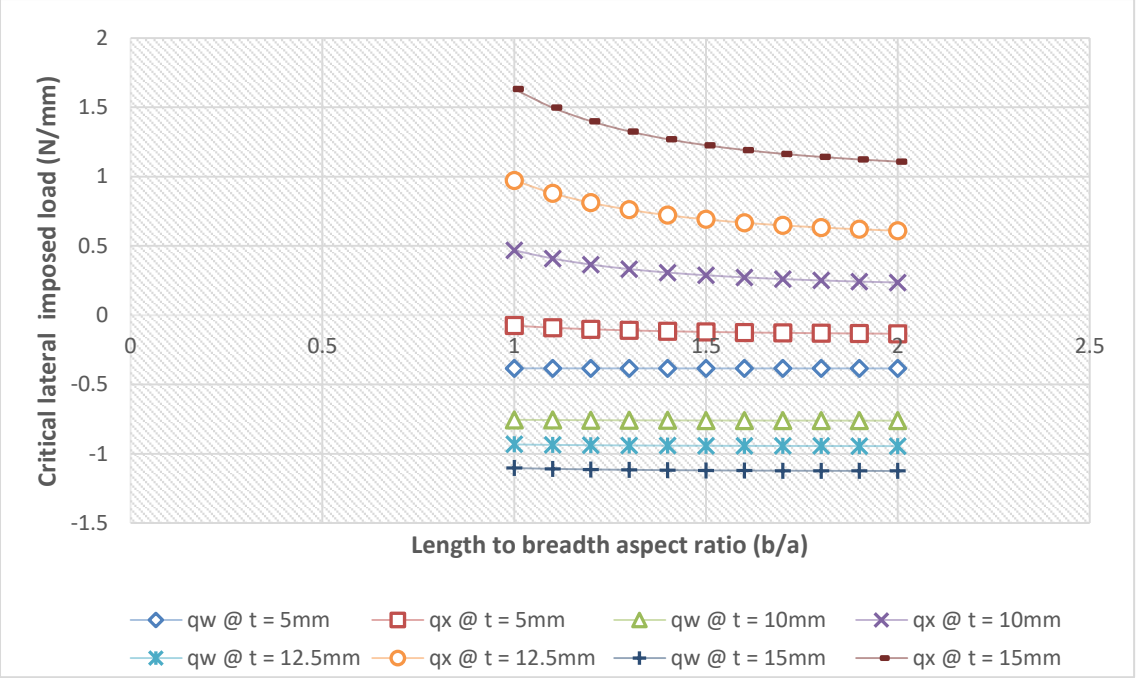

Figure 9: Graph of critical lateral imposed load versus length to breadth ratio of CSFS plate for span, a = 5000mm at $w_a = 3.0mm$

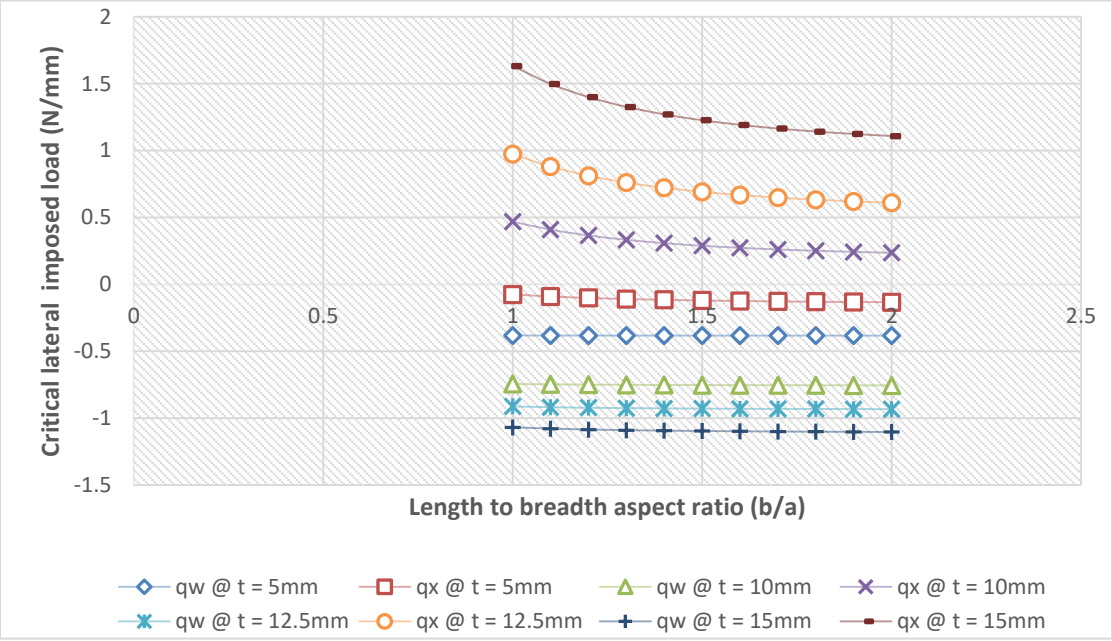

Figure 10: Graph of critical lateral imposed load versus length to breadth ratio of CSFS plate for span, a = 5000mm at $w_a = 5.0mm$

Similarly, Figure 11 (SCFC plate with span of 1000mm at allowable deflection (w_a) value between 1mm to 5mm). It is shown that failure neither occurs on q_{iw} *nor* q_{ip} at any thickness of and length to width ratio. This implies that the structure is safe.

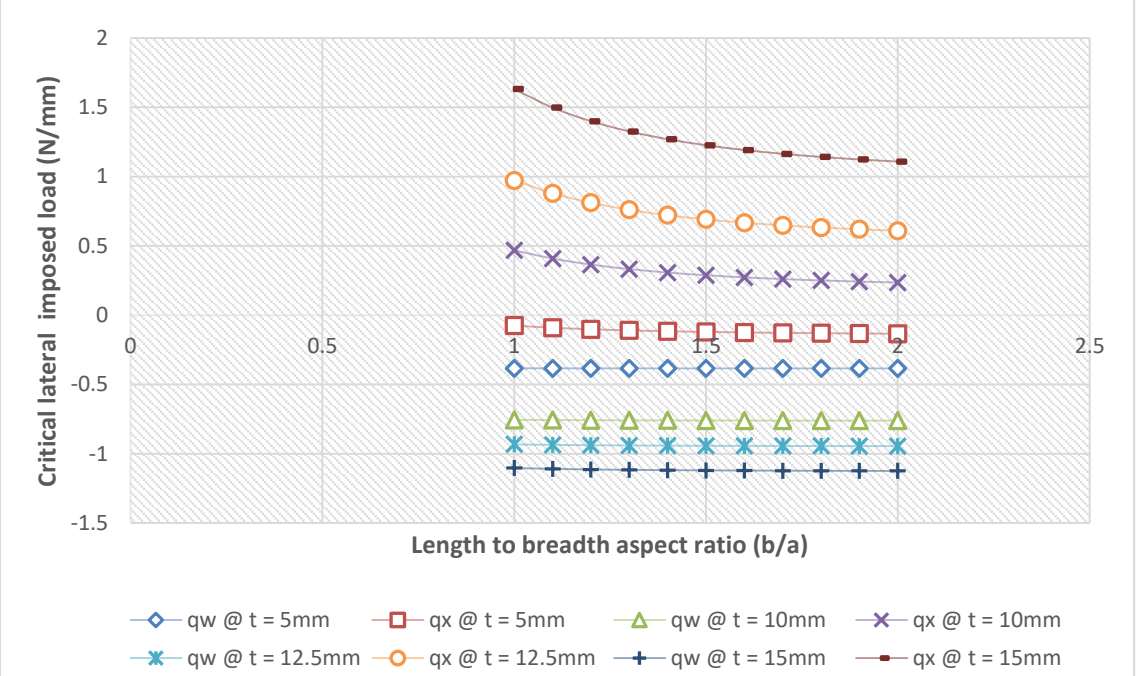

Figure 11: Graph of critical lateral imposed load versus length to breadth ratio of CSFS plate for span, a = 5000mm at $w_a = 3.0mm$

Looking closely at Figure 12 to 14 (SCFC plate with span between 1000mm and 5000mm at allowable deflection (w_a) value between 1mm to 5mm). It is finds that failure on q_{iw} only occurs at all length to width ratio (1 to 2) between value of -1.1125N/mm and -0.3717N/mm at all thickness. The negative value of critical lateral imposed load q_{iw} (and positive value of q_{ip}) only reveals that the plate fails in q_{iw} for the entire plate w_a (5mm to 15mm) and span of 3000mm to 5000mm. This means that the plate structure is not safe and required maintenance.

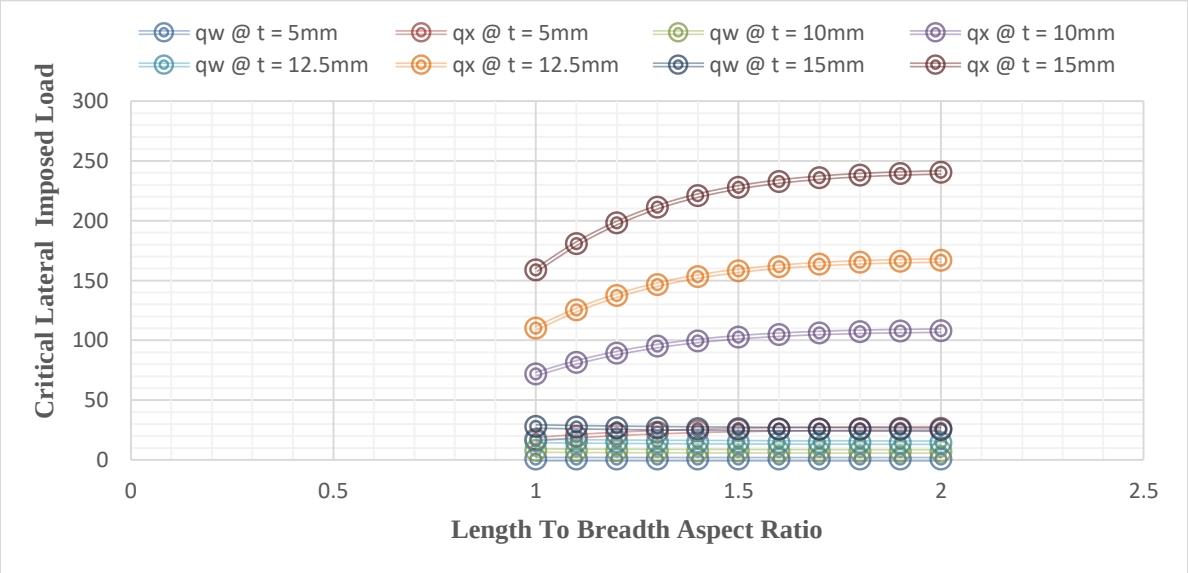

Figure 12: Graph of critical lateral imposed load versus length to breadth ratio of SCFC plate for span, a = 1000mm at $w_a = 1.0mm$

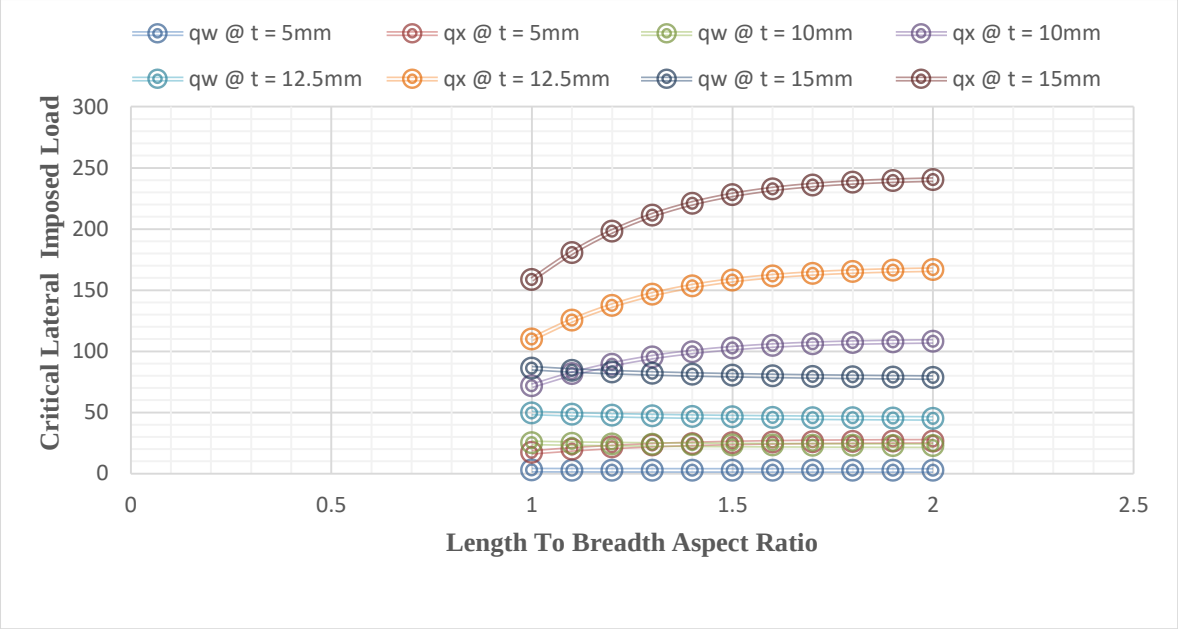

Figure 13: Graph of critical lateral imposed load versus length to breadth ratio of SCFC plate for span, a = 1000mm at $w_a = 3.0mm$

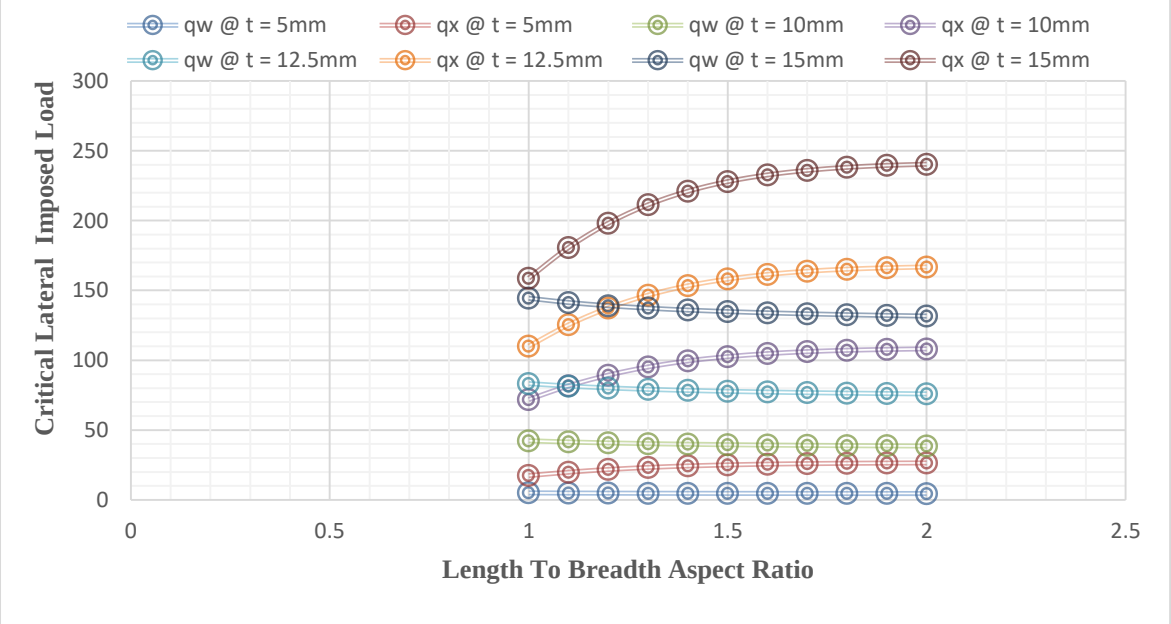

Figure 14: Graph of critical lateral imposed load versus length to breadth ratio of SCFC plate for span, a = 1000mm at $w_a = 5.0mm$

From that table it is observed that the value of q_{ip} if greater than that of q_{iw}, this is because the failure of plate in q_{ip} means total failure, but that of q_{iw} is like a warning requesting maintenance.

The positive value of critical lateral imposed load q_{iw} *and* q_{ip} for other types of plate reveals that the plate neither fail in q_{iw} nor in q_{ip} for plate all span at allowable deflection, w_a of 1000mm to 5000mm for the two boundary conditions into consideration. This means that the plate structure is safe.

7. CONCLUSION

It is concluded that the values of critical lateral load obtained by this theory achieve accepted vertical shear stress to the thickness of plate variation and satisfied the transverse flexibility of condition of the plate while predicting the bending behavior of an isotropic rectangular CSFS and SCFC plate.

Conflict of Interest Statement

On behalf of all authors, I Onyeka Festus the corresponding author hereby state that there is no conflict of interest.

References

[1]. Pagano N. J., (1967). Exact solutions for composite laminates in cylindrical bending. *J Compos Mater*, Vol. *3*: 398–411.

[2]. Pipes RB, Pagano N. J., (1970). Interlinear stresses in composite laminates under axial extension. *J Compos Mater*, Vol. 4: 538–648.

[3]. Ghugal, Y. M. and Sayyad, A.S., (2011). Free vibration of thick isotropic plates using trigonometric shear deformation theory. *J. Solid Mech*. Vol. 3(2): 172-182.

[4]. Mantari, A.S. Oktem, C. Guedes Soares., (2012). A new trigonometric shear deformation theory for isotropic, laminated composite and sandwich plates. *Int. J. Solids and Struc*, Vol. 49: 43-53.

[5]. Mindlin, R. D., (1951). Influence of rotary inertia and shear on flexural motions of isotropic, elastic plates. *ASME Journal Applied Mechanics*, Vol. 18: 31–38.

[6]. Ghugal, Y. M., Kulkarni, S. K., (2011). Thermal stress analysis of cross-ply laminated plates using refined shear deformation theory. *Journal of Experimental and Applied Mechanics*, Vol. 2: 47–66.

[7]. Reddy J. N., (1984). A refined non-linear theory of plates with transverse shear deformation. *International Journal of Solids and Structures*, Vol. 20: 881-896.

[8]. Sayyad, A. S., Ghugal, Y. M., (2012). Bending and free vibration analysis of thick isotropic plates by using exponential shear deformation theory. *Applied and Computational Mechanics*, Vol. 6(1): 65–82.

[9]. Sayyad, A. S., Ghugal, Y. M., (2012). Buckling analysis of thick isotropic plates by using exponential shear deformation theory. *Applied and Computational Mechanics*, Vol. 6(2): 185–196.

[10]. Reissner, E., (1945). The effect of transverse shear deformations on the bending of elastic plates. *ASME Journal of Applied Mechanics*. Vol. 12: A69-A77.

[11]. Soldatos, K. P., (1992). A transverse shear deformation theory for homogeneous monoclinic plates. *Acta Mechanica*, Vol. 94: 195–200.

[12]. Soldatos, K. P., (1988). On certain refined theories for plate bending, *ASME Journal of Applied Mechanics*, Vol. 55: 994–995.

[13]. Onyeka, F. C., Okafor, F. O., Onah, H. N., (2018). Displacement and Stress Analysis in Shear Deformable Thick Plate, *International Journal of Applied Engineering Research*, Vol. 13(11): 9893-9908.

[14]. Onyeka, F.C (2019). Direct Analysis of Critical Lateral Load in a Thick Rectangular Plate using Refined Plate Theory, *International Journal of Civil Engineering and Technology* Vol. 10(5): 492-505.

[15]. Ibearugbulem, O. and Onyeka, F., (2020). Moment and Stress Analysis Solutions of Clamped Rectangular Thick Plate. *European Journal of Engineering Research and Science*, Vol. 5(4): 531-534.

[16]. Onyeka, F. C. and Ibearugbulem, O. M. (2020). Load analysis and bending solutions of rectangular thick plate. *International journal on emerging technologies*, 11(3): 1103–1110.

[17]. Kirchhoff, G. R. (1850). U''ber das Gleichgewicht and die Bewe gung einer elastschen Scheibe, *Journal f'' ur die reine und angewandte Mathematik*, 40: 51-88 (in German).

[18]. Kirchhoff, G. R. (1850). U''ber die Schwingungen einer kriesformigen elastischen Scheibe, *Annalen der Physik und Chemie*, 81: 258-264 (in German).